

---

# Combining observational datasets from multiple environments to detect hidden confounding

---

**Rickard K.A. Karlsson**  
Delft University of Technology  
The Netherlands  
r.k.a.karlsson@tudelft.nl

**Jesse H. Krijthe**  
Delft University of Technology  
The Netherlands  
j.h.krijthe@tudelft.nl

## Abstract

A common assumption in causal inference from observational data is the assumption of no hidden confounding. Yet it is, in general, impossible to verify the presence of hidden confounding factors from a single dataset. However, under the assumption of independent causal mechanisms underlying the data generative process, we demonstrate a way to detect unobserved confounders when having multiple observational datasets coming from different environments. We present a theory for testable conditional independencies that are only violated during hidden confounding and examine cases where we break its assumptions: degenerate & dependent mechanisms, and faithfulness violations. Additionally, we propose a procedure to test these independencies and study its empirical finite-sample behavior using simulation studies.

## 1 Introduction

Estimating the causal effect of a treatment on an outcome is a fundamental challenge in many areas of science and society. While this is straightforwardly done using data from randomized studies, using observational data for this task is appealing since they are often more feasible to collect while also being more representative of the population of interest (Pearl, 2009). To identify causal effects using such data it is often assumed there is no hidden confounding. When this untestable assumption is violated we run the risk of confusing causal relationships with spurious correlations. This can have serious consequences such as unknowingly giving a non-effective or, even worse, potentially harmful treatment to a patient. Therefore, detecting the presence of hidden confounding is an important problem.

Observational data tends to be heterogeneous due to e.g. changing circumstances or time-shifts in distributions. In this work, we show how this heterogeneity can be exploited to make hidden confounding testable: we show that using data from multiple heterogeneous environments allows us to detect hidden confounding in observational data.

We consider a setting where observational data has been collected from different environments where the same treatment  $T$  and outcome  $Y$  have been observed. Further, we assume that the data is heterogeneous across these environments under the principle of *Independent Causal Mechanisms* (Peters et al., 2017), which states that a causal system consists of autonomous modules that do not inform or influence each other. The question we ask is whether there exists hidden confounding between  $T$  and  $Y$  as visualized in Figure 1. If that is the case, the causal effect of  $T$  on  $Y$  is not identifiable

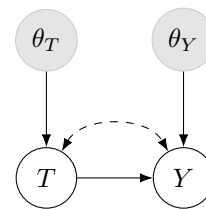


Figure 1: Data generating process with independent causal mechanisms  $\theta_T$  and  $\theta_Y$ ; gray indicates unobserved variables. The dashed bi-directed edge represents possible hidden confounding between  $T$  and  $Y$ .

in general. Perhaps surprisingly, we demonstrate that we can sometimes answer this question using testable implications of the independent causal mechanism principle in this setting.

For example, imagine a situation where we have collected observational data for a specific treatment and outcome from multiple hospitals that care for patients in different demographics. As a consequence, we might suspect the existence of potential confounders such as income status or health seeking behavior. If these factors have different distributions at each hospital, our work proposes a way to statistically test the presence of confounding, even when we do not observe the confounding factors directly.

**Contributions** In this work, we present the assumptions and theory underpinning the testing of hidden confounding from combining datasets from multiple environments (Sec. 4.1, Theorem 1). In addition, we explore the effect of changes and violations of our assumptions (Sec. 4.2) and use simulation studies for an empirical finite-sample analysis of a proposed statistical testing procedure (Sec. 5).

## 2 Problem Setting

Assume  $T \in \mathcal{T}$  is the treatment and  $Y \in \mathcal{Y}$  is the outcome of interest with a joint distribution  $T, Y \sim P(T, Y)$ . In addition, we assume to sample data from different environments  $E \in \mathcal{E} = \{e_1, e_1, \dots, e_K\}$  which have the distribution  $T^{(k)}, Y^{(k)} \sim P(T, Y \mid E = e_k)$  for  $k = 1, \dots, K$ . Within each environment, the sampled data is assumed to be i.i.d..

Expressed in the framework of Pearl (2009), our goal in causal inference is to estimate the probability  $P(Y \mid do(T = t))$  where  $do(T = t)$  represents an intervention on the treatment. Without any further assumptions,  $P(Y \mid do(T = t))$  is not identifiable from an observational dataset; that is data where we have observed the choice of treatment without influencing it. In fact, when  $T \not\perp\!\!\!\perp Y$  there are three possible explanations under the assumption of no selection bias that would lead to vastly different conclusions about  $P(Y \mid do(T = t))$ : (i)  $T$  is a cause of  $Y$ , (ii)  $Y$  is a cause of  $T$  or (iii) they are dependent through a hidden confounder<sup>1</sup>, which we denote with  $U \in \mathcal{U}$ .

Things change when we have access to datasets from multiple environments. Then, we can discriminate between the three different causal explanations for  $T \not\perp\!\!\!\perp Y$ . Guo et al. (2022) showed how to distinguish between  $T$  being a cause of  $Y$  and  $Y$  being a cause of  $T$ , but left the existence of a common cause as an open question. We resolve this question, hence demonstrating a novel and valuable approach for causal inference from observational data.

## 3 Related Work

In this work, we use the principle of *Independent Causal Mechanisms* (Peters et al., 2017). It states that a causal system comprises autonomous modules that do not inform or influence each other, and it has inspired further research on integrating machine learning and causality (Schölkopf et al., 2012; Peters et al., 2016; von Kügelgen et al., 2020; Schölkopf et al., 2021). Recently, Guo et al. (2022) drew parallels to de Finetti’s theorem (de Finetti, 1937) about the existence of independent causal mechanisms when the data is an infinitely exchangeable sequence. Moreover, both Zhang et al. (2017) and Guo et al. (2022) demonstrate how the independent causal mechanism principle could improve causal structure learning when data comes from heterogeneous environments that share the same causal model. Our work continues on these developments to detect hidden confounding.

Combining data from multiple environments to learn causal structures has also been studied by Mooij et al. (2020), who developed a principled framework dubbed *Joint Causal Inference* (JCI). When having contextual information on how variables in the data varies separately across environments, they demonstrate how to apply traditional constraint-based methods for causal discovery (Glymour et al., 2019) to the combined data. In our setting with observed variables  $(T, Y, E)$ , the JCI framework demonstrate that  $Y \perp\!\!\!\perp E \mid T$  is violated in the presence of hidden confounding under the assumption that  $P(T \mid E)$  varies across environments. This test has also been mentioned by Athey et al. (2020, Lemma 3). Unlike the condition we propose in this work, this alternative test requires that  $P(Y \mid T, E)$  is constant with respect to  $E$  since the converse would break the independence. Our

<sup>1</sup>This is known as Reichenbach’s common cause principle (Reichenbach, 1956).

contribution, presented in Theorem 1, is a more general test that works under any environmental change.

Various approaches have been proposed to deal with hidden confounding when having access to multiple environments, typically by combining both experimental and observational data (Bareinboim and Pearl, 2016; Kallus et al., 2018; Athey et al., 2020; Hatt et al., 2022; Ilse et al., 2022). Bareinboim and Pearl (2016) give a general framework to estimate the causal effect, whenever it is identifiable, with data from different heterogeneous domains. Kallus et al. (2018) does not assume to have observed all confounders in an observational dataset under the condition that it is possible to use a separate experimental dataset to effectively model the confounding bias. Imbens et al. (2022) show how to correct for confounding bias when the treatment effect on a primary outcome is completely mediated through intermediary outcomes which are observed in different datasets. Similar to the above body of work, we also strive to deal with hidden confounding but our approach differs in two ways: firstly, our goal is to directly detect hidden confounding and, secondly, our procedure does not assume availability of experimental data.

#### 4 Detecting hidden confounding from heterogeneous environments

We use the Independent Causal Mechanism principle to reason formally about heterogeneity in our data distribution. Consider the joint density over a directed acyclic causal graph which can be factorized into conditional probabilities

$$P(X_1, X_2, \dots, X_k) = \prod_{i=1}^k P(X_i | \text{Pa}(X_i))$$

where  $\text{Pa}(X_i)$  denotes the parents of  $X_i$ . Then, intuitively, the principle states that these conditional probabilities represent causal mechanisms that are independent of each other (Peters et al., 2017).

**Assumption 1** (Independent Causal Mechanisms (Peters et al., 2017)). *The causal generative process of a system’s variables is composed of autonomous modules that do not inform or influence each other. In the probabilistic case, this means that the conditional distribution of each variable given its causes (i.e., its parents in the causal graph) does not inform or influence the other mechanisms.*

Returning to our setting with treatment  $T$ , outcome of interest  $Y$  and a possible latent confounder  $U$ , we assume they share the same acyclic causal graph across multiple environments with independent causal mechanisms. We parameterize their respective causal mechanisms with  $\theta_T \in \mathcal{V}_T$ ,  $\theta_U \in \mathcal{V}_U$  and  $\theta_Y \in \mathcal{V}_Y$ . These relationships can be described with the causal graph as seen in Figure 2. Additionally, we assume that the independent causal mechanisms have non-degenerate probability measures for each independent causal mechanism. Together with Assumption 1, it follows that  $\theta_T$ ,  $\theta_U$  and  $\theta_Y$  are pairwise independent random variables.

**Assumption 2** (Non-degenerate independent causal mechanisms). *The independent causal mechanisms are non-degenerate random variables with probability measures  $P(\theta_T)$ ,  $P(\theta_U)$  and  $P(\theta_Y)$ .*

Although we explicitly assume independent causal mechanisms with non-degenerate probability measures, Guo et al. (2022) proved the existence of these when the data comprises an infinitely exchangeable sequence of categorical random variables. We, however, allow any type of distribution in Assumption 2.

**Sampling from different environments** With the random independent causal mechanisms, we can formally describe the sampling procedure of  $(T, Y, E)$  from different environments sharing the same causal model.

We define the environment variable as  $E = (\theta_T, \theta_U, \theta_Y)$ , the tuple of the random independent causal mechanisms. We obtain different environments by sampling according to  $E \sim P(E) =$

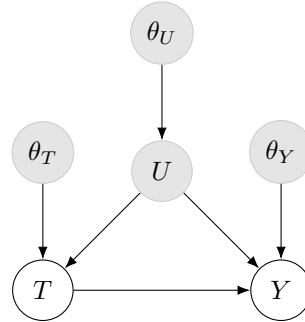


Figure 2: The data generating process for  $T$  and  $Y$ , explicitly including a confounder  $U$ , together with their respective causal mechanisms. Gray indicates unobserved variables.

$P(\theta_T)P(\theta_U)P(\theta_Y)$  and obtain a set of tuples  $\mathcal{E} = \{(\theta_T^{(1)}, \theta_U^{(1)}, \theta_Y^{(1)}), \dots, (\theta_T^{(K)}, \theta_U^{(K)}, \theta_Y^{(K)})\}$  where we let  $e_i = (\theta_T^{(i)}, \theta_U^{(i)}, \theta_Y^{(i)})$  for  $i = 1, 2, \dots, K$ . In each environment  $e_i$ , the distribution  $P(T, Y | E = e_i)$  may change depending on the values of  $(\theta_T^{(i)}, \theta_U^{(i)}, \theta_Y^{(i)})$  which leads to heterogeneity across environments. For instance, under presence of the confounder  $U$ , we could have  $T = \beta U + \varepsilon$  where  $\varepsilon \sim N(0, \sigma^2)$  and then let  $\theta_T = (\beta, \sigma)$  vary across different environments.

Finally, the observed data is sampled from the different environments,

$$T^{(i)}, Y^{(i)} \sim P(T, Y | E = e_i), \quad i = 1, \dots, K.$$

Note that we require to know which environment a particular sample comes from, but we do not necessarily know the values of  $(\theta_T^{(i)}, \theta_U^{(i)}, \theta_Y^{(i)})$  in the environments.

#### 4.1 Testable conditional independencies

Our goal is to detect the existence of latent confounding between treatment  $T$  and outcome  $Y$ . Graphically, this corresponds to detecting the edges  $U \rightarrow T$  and  $U \rightarrow Y$ . In this section, we demonstrate testable conditional independencies that are only violated when both those edges exist. Note that, for clarity, we explicitly write out  $U$  although it is not an observed variable.

**Comparing samples across environments** Let  $\mathbf{T} = (T_1, T_2, \dots, T_N)$  be a row vector containing  $N$  samples where  $T_i$  is the  $i$ th sample, and define  $\mathbf{Y}, \mathbf{U}$  similarly. In our setting, we note that the joint probability distribution over sampled datasets  $(\mathbf{T}, \mathbf{Y}, \mathbf{U})$  can be factorized as:

$$\begin{aligned} P(\mathbf{T}, \mathbf{Y}, \mathbf{U}) &= \int_{\mathcal{V}_T, \mathcal{V}_Y, \mathcal{V}_U} P(\mathbf{Y} | \mathbf{T}, \mathbf{U}, \theta_Y) P(\mathbf{T} | \mathbf{U}, \theta_T) P(\mathbf{U} | \theta_U) dP(\theta_T) dP(\theta_U) dP(\theta_Y) \\ &= \int_{\mathcal{V}_T, \mathcal{V}_Y, \mathcal{V}_U} \prod_{i=1}^N P(Y_i | T_i, U_i, \theta_Y) P(T_i | U_i, \theta_T) P(U_i | \theta_U) dP(\theta_T) dP(\theta_U) dP(\theta_Y) \end{aligned}$$

where we marginalize over the causal mechanisms in the first equality and then obtain the second equality by noting that all samples are i.i.d. when conditioned on the environment  $E = (\theta_T, \theta_U, \theta_Y)$ . This factorization can be represented as the graph in Figure 3, for which we only included two different samples  $i$  and  $j$  for illustration.

We use the graph in Figure 3 for reasoning to reach our original goal: to detect hidden confounding. Notably, the graph displays open paths between  $T_i$  and  $Y_j$  that goes through both edges  $U \rightarrow T$  and  $U \rightarrow Y$ . If either of these edges did not exist then there would be no hidden confounding from  $U$ . As we show, there is a complete set of conditional independencies corresponding to open paths going through those edges.

But first, we state our final assumption that the causal graphs correctly represents the underlying data distribution, as formalized with the faithfulness and causal Markov property assumption.

**Assumption 3** (Faithfulness and causal Markov property). *The data distribution  $P(X, Y, U, \theta_T, \theta_U, \theta_Y)$  and its underlying causal graph  $\mathcal{G}$  fulfill (i) the faithfulness property, independence relationships observed in  $P$  implies matching  $d$ -separations in  $\mathcal{G}$ , and (ii) the causal Markov property, independence relationships obtained from  $d$ -separation in  $\mathcal{G}$  also hold in  $P$ .*

We present our main theorem which proves testable conditional independencies for hidden confounding between the treatment  $T$  and outcome  $Y$  when we have data from multiple environments.

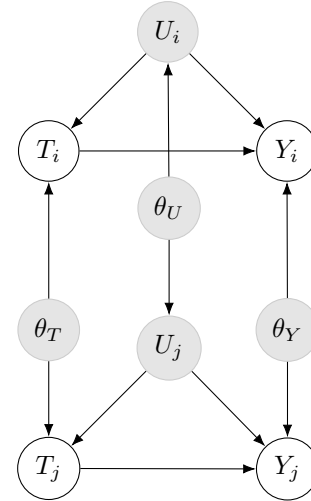


Figure 3: The causal graph with a confounder  $U$  between  $T$  and  $Y$  over a pair of samples  $(i, j)$ . Gray indicates unobserved variables.

**Theorem 1.** *Under assumption 1, 2 and 3, with datasets from distribution  $P(\mathbf{T}, \mathbf{Y}, \mathbf{U})$  that has an underlying acyclic causal graph with unknown edges, then:*

$$\begin{aligned} (i) \quad & T_j \not\perp\!\!\!\perp Y_i \mid T_i \text{ for } i \neq j \\ & \text{and} \qquad \qquad \qquad \iff U \text{ is a confounder to } T \text{ and } Y . \\ (ii) \quad & T_j \not\perp\!\!\!\perp Y_i \mid Y_j \text{ for } i \neq j \end{aligned}$$

*In particular, the implications are testable without observing  $U$ .*

*Proof sketch.* To prove the statement, we go through all possible directed acyclic graphs with  $T$ ,  $Y$  and  $U$  as variables. With the independent causal mechanism principle, we obtain graphs as in Figure 3, for which we show that the implications in the theorem correspond to a class of graphs where  $U$  is a common cause to both  $T$  and  $Y$ . The full proof can be found in the Appendix.  $\square$

The interpretation of the theorem is that for a causal graph with the variables  $T, Y, U$ , we have testable implications for whether  $U$  has any directed edges into both  $T$  and  $Y$  no matter what the causal direction between  $T$  and  $Y$  is. Hence, assuming faithfulness, if  $T_j \perp\!\!\!\perp Y_i \mid T_i$  or  $T_j \perp\!\!\!\perp Y_i \mid Y_j$  then there is no confounding between  $T$  and  $Y$ .

In practice, we may often know if a treatment  $T$  happens before  $Y$  in time; implying that  $T$  can not be a descendant of  $Y$  in a causal graph. If this is the case, only one of the conditions in Theorem 1 is sufficient to detect hidden confounding, as described by the following corollary.

**Corollary 1.** *In addition to having the same data and assumptions as in Theorem 1, if we have that  $T$  is not a descendant of  $Y$ , then the following holds:*

$$(i) \quad T_j \not\perp\!\!\!\perp Y_i \mid T_i \text{ for } i \neq j \iff U \text{ is a confounder to } T \text{ and } Y .$$

Similarly, if we instead would assume that  $T$  is an ancestor of  $Y$ , we only need condition (ii) from Theorem 1, that is  $T_j \not\perp\!\!\!\perp Y_i \mid Y_j$ , to detect confounding.

## 4.2 Influence of the Assumptions

The implications in Theorem 1 can be used to test hidden confounding, but they are not a silver bullet since they rely on other untestable assumptions, namely non-degenerate independent causal mechanism, and the faithfulness & causal Markov property. Due to this, we investigate the necessity of these assumptions and identify various failure cases where they are violated. But also, on a more positive note, we demonstrate that the assumption of non-degenerate mechanisms can be weakened.

**Violation of Assumption 1: dependent causal mechanisms** What happens if either  $\theta_T \perp\!\!\!\perp \theta_U$ ,  $\theta_T \perp\!\!\!\perp \theta_Y$  or  $\theta_U \perp\!\!\!\perp \theta_Y$  are violated? To investigate this, we go through the same procedure for proving Theorem 1 with the difference that we allow any of these mechanisms to be dependent. In all cases, Theorem 1 and Corollary 1 fails since their conditional independencies no longer imply no confounding. An example of this can be found in the Appendix. We conclude that the independent causal mechanism assumption is indeed necessary.

**Violation of Assumption 2: degenerate causal mechanisms** What happens if one or more of the distributions  $P(\theta_T)$ ,  $P(\theta_U)$  and  $P(\theta_Y)$  are constant across all environments? We investigate these scenarios by first adding  $\theta_T$ ,  $\theta_U$  and/or  $\theta_Y$  to the conditioning set of the independencies in Theorem 1. Then, we check whether these independencies still are violated in the presence of hidden confounding using the same procedure as for proving the theorem.

Out of seven possible cases with degenerate mechanisms, we identify three where Theorem 1 fails: when either  $\{\theta_T, \theta_U\}$ ,  $\{\theta_U, \theta_Y\}$  or  $\{\theta_T, \theta_U, \theta_Y\}$  are degenerate together. The reason  $\theta_T$  and  $\theta_U$  can not be degenerate together is that condition (i) no longer exclusively holds when there is confounding. Similarly, condition (ii) breaks when  $\theta_U$  and  $\theta_Y$  are degenerate together.

Hence, for Corollary 1, where only condition (i) appears, it is sufficient for just  $\theta_T$  or  $\theta_U$  to be non-degenerate. Interestingly, this can be verified by checking that  $P(T \mid E)$  varies across environments, which also coincides with the necessary condition for the previously mentioned approach of testing  $Y \perp\!\!\!\perp E \mid T$  to detect confounding (Mooij et al., 2020; Athey et al., 2020).

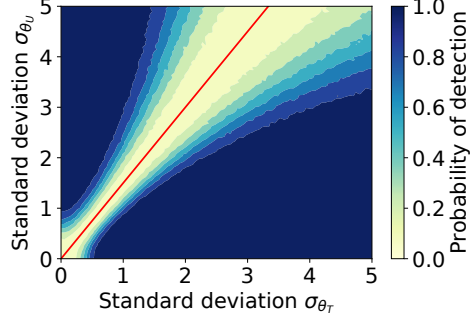


Figure 4: Faithfulness violation from Example 1: Varying  $\sigma_{\theta_T}$  and  $\sigma_{\theta_U}$  with  $\sigma_T = \frac{2}{3}$  and  $\sigma_U = 1$ , probability for detecting confounding goes to zero as we get closer to  $\sigma_{\theta_U} = \frac{\sigma_U}{\sigma_T} \sigma_{\theta_T}$  (red line).

**Violation of Assumption 3: faithfulness violation** What happens if the conditional independencies in Theorem 1 do not correspond to the dependencies in the underlying causal graph? If that is the case, we would fail to detect dependencies implying the presence of confounders. Knowing when a faithfulness violation occurs is not possible, we can only reason about its plausibility.

It was proved by Meek (1995) that all graphs with discrete and linear-Gaussian data distributions fulfill faithfulness in a measure-theoretic sense; distributions that violate faithfulness have measure zero. However, even if we restrict  $T$  and  $Y$  to be categorical we might not want to assume that  $U$  or the causal mechanisms follow a discrete distribution. The following example also demonstrates the practical issues stemming from faithfulness violations even when the data is jointly Gaussian.

**Example 1.** Consider the structural causal model

$$\begin{aligned} U &= \theta_U + \varepsilon_U, & \varepsilon_U &\sim \text{Normal}(0, \sigma_U^2), \\ T &= U + \theta_T + \varepsilon_T, & \varepsilon_T &\sim \text{Normal}(0, \sigma_T^2), \\ Y &= U + T + \theta_Y + \varepsilon_Y, & \varepsilon_Y &\sim \text{Normal}(0, \sigma_Y^2), \end{aligned} \quad (1)$$

where  $\theta_T \sim \text{Normal}(0, \sigma_{\theta_T}^2)$ ,  $\theta_U \sim \text{Normal}(0, \sigma_{\theta_U}^2)$  and  $\theta_Y \sim \text{Normal}(0, \sigma_{\theta_Y}^2)$ . We have that  $\varepsilon_c \perp\!\!\!\perp \theta_c$  for  $c = T, Y, U$ . Then, despite the presence of confounding,  $T_j \perp\!\!\!\perp Y_i \mid T_i$  for any  $i \neq j$  when  $\sigma_{\theta_U} = \frac{\sigma_U}{\sigma_T} \sigma_{\theta_T}$ . Interestingly, in the finite-sample setting, it noticeably influences our ability to detect confounding when the distribution parameters come close to this equality, as illustrated in Figure 4. A full derivation of this example can be found in the Appendix.

### 4.3 Statistical Testing Procedure

Testing the conditional independencies in Theorem 1 requires only two observed samples  $(i, j)$  per environment where  $i, j \in \{1, \dots, N\} : i \neq j$ . In this section, we describe a testing procedure which exploits that we may observe more than two samples per environment.

We mainly discuss the case where the treatment and outcome are binary or categorical because it (i) is a common scenario in causal inference and (ii) already provides practical challenges in our setting that need to be resolved. In the following, we consider the task of testing the conditional independence  $T_j \perp\!\!\!\perp Y_i \mid T_i$  as in Corollary 1, which is sufficient to detect confounding assuming that  $T$  is not be caused by  $Y$ . For simplicity, we assume to have the same number of samples per environment although this is not required.

**Multiple contingency table tests** For a given pair of samples  $i$  and  $j$ , we want to test whether  $T_j \perp\!\!\!\perp Y_i \mid T_i$  is true. In this case, the data consists of  $Y_i$  and  $T_i$  which are vectors of length  $K$  comprising matching samples across all environments and  $T_j$  which is a vector of separate samples across all environments.

With categorical variables, we can use contingency table testing under the null hypothesis of independence; a popular alternative for this is the G-test (McDonald, 2014, pages 68-76). The G-test returns a test statistic that is asymptotically  $\chi^2$ -distributed with  $(|\mathcal{T}| - 1) \cdot (|\mathcal{Y}| - 1)$  degrees of freedom. It can be used to test conditional independencies by computing its test statistic for each

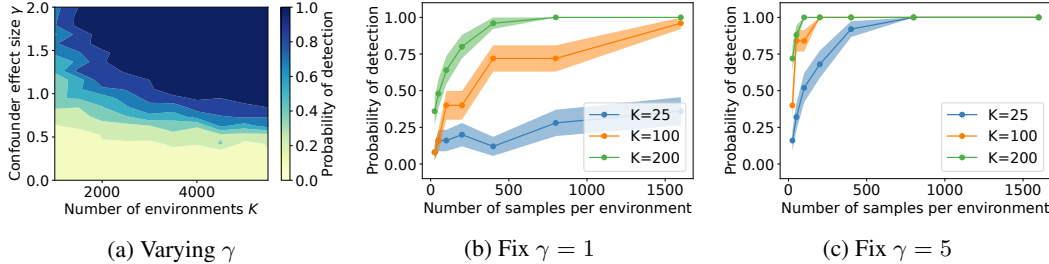


Figure 5: Probability of detecting hidden confounding for varying the number of environments  $K$  and samples per environments  $N$ . **(a)**: simulations with  $N = 2$  across a range of confounder effect sizes. **(b)**, **(c)**: simulations with permutation-based testing procedure for  $N > 2$  with a small number of environments  $K$ . Shaded area shows standard deviation from 25 iterations.

value of the conditioning variable, then the sum of these statistics also follow a  $\chi^2$  distribution. In our setting, we can do this test for every non-overlapping pair of samples  $(i, j)$  and, once more, check the  $\chi^2$ -distributed sum of test statistics over each pair.

Notably, the asymptotic distribution of the G-test depends on the number of environments and not the number of samples and, as a consequence, may break down when the number of environments is small. In those settings, we use the Monte-Carlo permutation testing procedure proposed by Tsamardinos and Borboudakis (2010) which approximates an exact statistical test.

For more details on the asymptotic G-test and permutation-based procedure see the Appendix.

## 5 Experiments

To evaluate and investigate the theory for testing hidden confounding in multiple environments, we perform a series of simulation studies with binary data. First, we investigate how the effect size of the confounding variable relates to the probability of detection. Secondly, we explore how our testing procedure depends on the number of available samples and environments. Lastly, we test the sensitivity of both the proposed procedure and an alternative testing approach to environmental change. Additional experiments with continuous data are available in the Appendix.

**Experimental setup** The experiments are implemented in Python<sup>2</sup>, using an implementation of the G-test from the package *pgmpy* (Ankan and Panda, 2015). Unless otherwise stated, each experiment is repeated 50 times where we use a significance level  $\alpha = 0.05$ . We only test the conditional independence  $T_j \perp\!\!\!\perp Y_i \mid T_i$  as in Corollary 1. Depending on the experiment, we state whether we use the asymptotic or permutation-based procedure described in Section 4.3.

**Synthetic data generation** We use the following data generating process:

$$\begin{aligned}
 U &\sim \text{Normal}(\theta_U, 1) & \theta_Y &\sim \text{Normal}(0, \sigma_{\theta_Y}^2), \\
 T &\sim \text{Ber}(\text{Sigm}(\gamma U + \theta_T)) & \theta_Y &\sim \text{Normal}(0, \sigma_{\theta_Y}^2), \\
 Y &\sim \text{Ber}(\text{Sigm}(\gamma U + T + \theta_Y)) & \theta_Y &\sim \text{Normal}(0, \sigma_{\theta_Y}^2),
 \end{aligned}
 \tag{2}$$

where  $\text{Sigm}(x) = 1/(1 + e^{-x})$  is the sigmoid function. Unless otherwise stated, we use  $\sigma_{\theta_U} = \sigma_{\theta_T} = \sigma_{\theta_Y} = 1$ . We control the strength of confounding by varying  $\gamma$ , where 0 corresponds to no confounding.

### 5.1 Results

**Larger confounder effect sizes increase probability of detection** We investigate how the effect size of the confounding variable influences our proposed testing procedure. We vary  $\gamma$  between 0 (no confounding) and 2 and also vary the number of environments. We perform this experiment with

<sup>2</sup>Code available at [github.com/RickardKarl/detect-hidden-confounding](https://github.com/RickardKarl/detect-hidden-confounding).

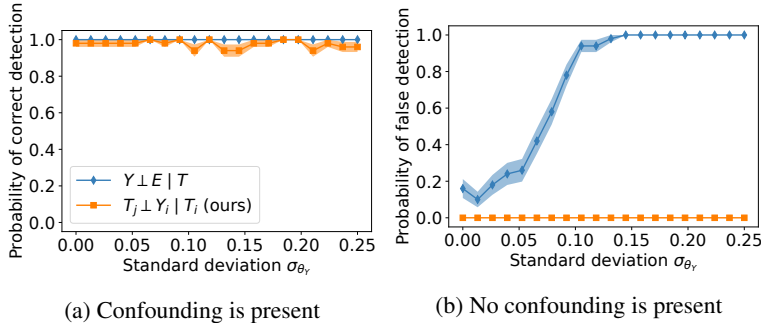


Figure 6: Comparing the proposed procedure and an alternative testing procedure by varying the standard deviation of  $\theta_Y$  in both the presence and absence of confounding

$N = 2$ . The results are shown in Figure 5a. We note two things: the probability of detection grows for larger confounder effect size and it also grows when the number of environments is increased.

**The growth rate in detection depends on the number of environments** We investigate the probability of detecting confounding when varying both the number of environments and number of samples per environment. We use the permutation-based testing procedure due to the limited number of environments.

The experiment shows that the testing procedure is highly dependent on the number of environments  $K$ , as illustrated in Figure 5b and 5c. For two different cases with either  $\gamma = 1$  or  $\gamma = 5$ , we note that the probability of detection grows as we increase the number of samples. Noticeably, the rate of growth increases with  $K$ , demonstrated with the difference between  $K = 200$  (—●—),  $K = 100$  (—●—) and  $K = 25$  (—●—). However, while for  $K = 25$  and  $\gamma = 5$  the probability converges to one with increasing sample size, we can not conclude anything about the case where  $\gamma = 1$ . As before, larger confounder effect size appears to make it easier to detect confounding. While our testing procedure successfully detects hidden confounding with a sufficient number of samples and environments, in particular the rate of convergence seems to improve greatly by adding more environments.

**Robustness to environmental change** We compare our procedure with testing the independence  $Y \perp E \mid T$  which only holds if there is no confounding. However, the latter assumes that  $P(Y \mid T, E)$  is constant across environments. Here we test the sensitivity to violating this condition. We vary  $\sigma_{\theta_Y}$  between 0 and  $\frac{1}{4}$  for both  $\gamma = 0$  (no confounding) and  $\gamma = 1$  (confounding) with  $N = 100$  and  $K = 500$ .

In the presence of confounding with  $\sigma_{\theta_Y} = 0$  both tests successfully detect confounding, as displayed in Figure 6a. Meanwhile, when there is no confounding and  $\sigma_{\theta_Y}$  starts to increase, the probability of false detection using  $Y \perp E \mid T$  increases while it remains close to zero for our procedure, this is shown in Figure 6b. We conclude that our procedure is more suitable when we can not assume that  $P(Y \mid T, E)$  stays unchanged across environments.

## 6 Discussion

In this work, we studied a setting where observational data has been collected from different heterogeneous environments in which the same treatment  $T$  and outcome  $Y$  have been observed. We showed that, under the principle of independent causal mechanisms, there exist testable conditional independencies that are violated in the presence of hidden confounders. On top of that, we investigated various failure cases and proposed a statistical procedure which we analyzed using simulation studies. In many cases, with a sufficient number of environments, we show that we are able to detect confounding when it is present and we demonstrate the benefit of our procedure compared to testing  $Y \perp E \mid T$  in the case that  $P(Y \mid T, E)$  varies across environments.

We have identified a set of open questions deriving from our work. Firstly, one can ask what the effect is on the theory when we have observed some confounders. If the hidden confounder  $U$  is independent of the observed confounder, then our procedure can be adapted to detect  $U$ . Another interesting

setting is when we observe a proxy to a hidden confounder, which can be used for adjustment instead (Kuroki and Pearl, 2014; Miao et al., 2018). In this case, it is no longer straightforward to say whether there could be a hidden confounder which is unrelated to the proxy.

Secondly, our theorem fundamentally relies on a set of untestable assumptions: independent & non-degenerate causal mechanisms and the faithfulness & causal Markov property. Although we investigated various violations, these results raised new questions. In particular, the effect of faithfulness violations, perhaps surprisingly, had a large influence on our procedure. Therefore, it is important to understand whether similar observations can be made in more realistic settings.

Thirdly, an interesting direction for future research would be to investigate how our approach can be used to estimate confounding strength, to be used in well-studied approaches in sensitivity analysis (Rosenbaum and Rubin, 1983; Cinelli et al., 2019).

Lastly, while our goal was to derive testable implications of hidden confounding, we observed that our proposed procedure requires a large number of environments to work well. It is unclear whether this is a property of the theory or the lack of efficiency in the test procedure we used. Since real-world datasets might have limited numbers of environments, more efficient testing procedures are needed, where a possible direction is to investigate how to improve upon the sample pair splitting which we currently do. A related but equally important problem is to also define efficient testing procedures for continuous or mixed continuous/categorical data.

## References

- Ankur Ankan and Abinash Panda. pgmpy: Probabilistic graphical models using python. In *Proceedings of the 14th Python in Science Conference (SCIPY 2015)*. Citeseer, 2015.
- Susan Athey, Raj Chetty, and Guido Imbens. Combining Experimental and Observational Data to Estimate Treatment Effects on Long Term Outcomes. *arXiv preprint arXiv:2006.09676*, 2020.
- Kunihiro Baba, Ritei Shibata, and Masaaki Sibuya. Partial correlation and conditional correlation as measures of conditional independence. *Australian & New Zealand Journal of Statistics*, 46(4): 657–664, 2004.
- Elias Bareinboim and Judea Pearl. Causal inference and the data-fusion problem. *Proceedings of the National Academy of Sciences*, 113(27):7345–7352, 2016.
- Carlos Cinelli, Daniel Kumor, Bryant Chen, Judea Pearl, and Elias Bareinboim. Sensitivity analysis of linear structural causal models. In *International conference on machine learning*, pages 1252–1261. PMLR, 2019.
- Bruno de Finetti. La prévision : ses lois logiques, ses sources subjectives. *Annales de l’institut Henri Poincaré*, 7(1):1–68, 1937.
- Clark Glymour, Kun Zhang, and Peter Spirtes. Review of causal discovery methods based on graphical models. *Frontiers in Genetics*, 10, 2019. ISSN 1664-8021.
- Siyuan Guo, Viktor Tóth, Bernhard Schölkopf, and Ferenc Huszár. Causal de Finetti: On the Identification of Invariant Causal Structure in Exchangeable Data. *arXiv preprint arXiv:2203.15756*, 2022.
- Tobias Hatt, Jeroen Berrevoets, Alicia Curth, Stefan Feuerriegel, and Mihaela van der Schaar. Combining Observational and Randomized Data for Estimating Heterogeneous Treatment Effects. *arXiv preprint arXiv:2202.12891*, 2022.
- Maximilian Ilse, Patrick Forré, Max Welling, and Joris M. Mooij. Combining Interventional and Observational Data Using Causal Reductions. *arXiv preprint arXiv:2103.04786*, 2022.
- Guido Imbens, Nathan Kallus, Xiaojie Mao, and Yuhao Wang. Long-term Causal Inference Under Persistent Confounding via Data Combination. *arXiv preprint arXiv:2202.07234*, 2022.
- Nathan Kallus, Aahlad Manas Puli, and Uri Shalit. Removing Hidden Confounding by Experimental Grounding. In *Advances in Neural Information Processing Systems*, volume 31. Curran Associates, Inc., 2018.
- Manabu Kuroki and Judea Pearl. Measurement bias and effect restoration in causal inference. *Biometrika*, 101(2):423–437, 2014. ISSN 0006-3444.
- J.H. McDonald. *Handbook of Biological Statistics*. Sparky House Publishing, 3rd edition, 2014.

- Christopher Meek. Strong completeness and faithfulness in bayesian networks. In *Proceedings of the Eleventh Conference on Uncertainty in Artificial Intelligence, UAI'95*, page 411–418, San Francisco, CA, USA, 1995. Morgan Kaufmann Publishers Inc. ISBN 1558603859.
- Wang Miao, Zhi Geng, and Eric J Tchetgen Tchetgen. Identifying causal effects with proxy variables of an unmeasured confounder. *Biometrika*, 105(4):987–993, 2018. ISSN 0006-3444.
- Joris M. Mooij, Sara Magliacane, and Tom Claassen. Joint causal inference from multiple contexts. *Journal of Machine Learning Research*, 21(99):1–108, 2020.
- Judea Pearl. *Causality*. Cambridge University Press, 2nd edition, 2009.
- Jonas Peters, Peter Bühlmann, and Nicolai Meinshausen. Causal inference by using invariant prediction: identification and confidence intervals. *Journal of the Royal Statistical Society: Series B (Statistical Methodology)*, 78(5):947–1012, 2016.
- Jonas Peters, Dominik Janzing, and Bernhard Schölkopf. *Elements of Causal Inference: Foundations and Learning Algorithms*. MIT Press, 1st edition, 2017.
- Hans Reichenbach. *The Direction of Time*. Dover Publications, 1956.
- P. R. Rosenbaum and D. B. Rubin. Assessing sensitivity to an unobserved binary covariate in an observational study with binary outcome. *Journal of the Royal Statistical Society. Series B (Methodological)*, 45(2):212–218, 1983. ISSN 00359246.
- Bernhard Schölkopf, Dominik Janzing, Jonas Peters, Eleni Sgouritsa, Kun Zhang, and Joris Mooij. On causal and anticausal learning. In *Proceedings of the 29th International Conference on International Conference on Machine Learning*, page 459–466. Omnipress, 2012. ISBN 9781450312851.
- Bernhard Schölkopf, Francesco Locatello, Stefan Bauer, Nan Rosemary Ke, Nal Kalchbrenner, Anirudh Goyal, and Yoshua Bengio. Toward causal representation learning. *Proceedings of the IEEE*, 109(5):612–634, 2021.
- Johannes Textor, Benito van der Zander, Mark S Gilthorpe, Maciej Liśkiewicz, and George TH Ellison. Robust causal inference using directed acyclic graphs: the R package ‘dagitty’. *International Journal of Epidemiology*, 45(6):1887–1894, 2017.
- Ioannis Tsamardinos and Giorgos Borboudakis. Permutation testing improves bayesian network learning. In José Luis Balcázar, Francesco Bonchi, Aristides Gionis, and Michèle Sebag, editors, *Machine Learning and Knowledge Discovery in Databases*, pages 322–337, Berlin, Heidelberg, 2010. Springer Berlin Heidelberg.
- Julius von Kügelgen, Alexander Mey, Marco Loog, and Bernhard Schölkopf. Semi-supervised learning, causality, and the conditional cluster assumption. In *Proceedings of the 36th Conference on Uncertainty in Artificial Intelligence (UAI)*, volume 124, pages 1–10. PMLR, 2020.
- Kun Zhang, Biwei Huang, Jiji Zhang, Clark Glymour, and Bernhard Schölkopf. Causal discovery from nonstationary/heterogeneous data: Skeleton estimation and orientation determination. In *Proceedings of the Twenty-Sixth International Joint Conference on Artificial Intelligence, IJCAI-17*, pages 1347–1353, 2017.

## Appendix

The appendix contains the following sections.

- A. **Proof of Theorem 1:** This section provides the full proof of Theorem 1.
- B. **Further analysis on the influence of the assumptions:** We elaborate on the examples of violating the assumptions behind our theory, as discussed in Section 4.2. First, we provide a concrete failure case when we have dependent causal mechanisms. Secondly, we demonstrate how we got to our conclusions on having degenerate mechanisms. Finally, we give a full derivation of Example 1 including additional insights on the asymptotic behavior of linear-Gaussian data with large confounder effect sizes.
- C. **Additional experiments:** We perform additional simulation studies, extending the results in the main paper with results with both continuous and binary data.
- D. **Algorithms:** We provide detailed algorithms to describe the two statistical testing procedures used in the main paper.

## A Proof of Theorem 1

In this section, we present the proof of the following theorem.

**Theorem 1.** Under assumption 1, 2 and 3, with datasets from distribution  $P(\mathbf{T}, \mathbf{Y}, \mathbf{U})$  that has an underlying acyclic causal graph with unknown edges, then:

$$\begin{aligned} (i) \quad T_j \not\perp\!\!\!\perp Y_i \mid T_i \quad \text{for } i \neq j \\ \text{and} \\ (ii) \quad T_j \not\perp\!\!\!\perp Y_i \mid Y_j \quad \text{for } i \neq j \end{aligned} \iff \text{U is a confounder to } T \text{ and } Y .$$

In particular, the implications are testable without observing  $U$ .

*Proof.* We go through all possible directed acyclic graphs (DAG) with  $T$ ,  $Y$  and  $U$  as variables. Under the assumption of non-degenerate, independent causal mechanisms (Assumption 1 and 2) we can construct graphs such as the one seen in Figure 3 where we consider every combination of the edges between  $T$ ,  $Y$  and  $U$  that lead to DAGs. In total, there are 25 different DAGs that encompass all these combinations of edges. We say that  $U$  is a confounder in one of these DAGs if both the edges  $U \rightarrow T$  and  $U \rightarrow Y$  exist.

Now, due to the assumption of non-degenerate mechanisms (Assumption 2), there exist open paths between any pair of samples  $(T_i, Y_i)$  and  $(T_j, Y_j)$  where  $i \neq j$  are two different sample indices. First, we check for what DAGs  $T_j \perp\!\!\!\perp_d Y_i \mid T_i$  and  $T_j \perp\!\!\!\perp_d Y_i \mid Y_j$  holds, where  $\perp\!\!\!\perp_d$  indicates d-separation (Pearl, 2009). This was done automatically using the *dagitty* package in R (Textor et al., 2017), the results are displayed in Table 1.

We note that the three first rows in Table 1 are the cases where  $U$  is a confounder, and these are the only cases where both  $T_j \perp\!\!\!\perp_d Y_i \mid T_i$  and  $T_j \perp\!\!\!\perp_d Y_i \mid Y_j$ . In other words, these two conditions are sufficient to determine whether  $U$  is a confounder. Assuming the faithfulness and causal Markov property (Assumption 3), we have that:

$$\begin{aligned} (i) \quad T_j \not\perp\!\!\!\perp_d Y_i \mid T_i \quad \text{for } i \neq j \\ \text{and} \\ (ii) \quad T_j \not\perp\!\!\!\perp_d Y_i \mid Y_j \quad \text{for } i \neq j \end{aligned} \iff \begin{aligned} (i) \quad T_j \not\perp\!\!\!\perp Y_i \mid T_i \quad \text{for } i \neq j \\ \text{and} \\ (ii) \quad T_j \not\perp\!\!\!\perp Y_i \mid Y_j \quad \text{for } i \neq j \end{aligned}$$

Consequently, it follows that

$$\begin{aligned} (i) \quad T_j \not\perp\!\!\!\perp Y_i \mid T_i \quad \text{for } i \neq j \\ \text{and} \\ (ii) \quad T_j \not\perp\!\!\!\perp Y_i \mid Y_j \quad \text{for } i \neq j \end{aligned} \iff \text{U is a confounder to } T \text{ and } Y .$$

□

**Remark** To prove Corollary 1 it is only necessary to look at the cases where  $Y$  is not an ancestor of  $T$  in Table 1 and recognize that  $T_j \not\perp\!\!\!\perp Y_i \mid T_i$  is then sufficient to identify cases where  $U$  is a confounder.



## B Further analysis on the influence of the assumptions

In this section, we present more elaboration on the examples of violating the assumptions behind our theory, as discussed in Section 4.2. First, we provide a counter-example which shows how Theorem 1 fails when we have dependent causal mechanisms. Secondly, we demonstrate how we got to our conclusions on having degenerate mechanisms. Finally, we give a full derivation to the Example 1 as well as additional insights on what can happen when the confounder effect sizes become very large.

### B.1 Dependent mechanisms

We wish to demonstrate examples of DAGs where condition (i) in Theorem 1, that is  $T_j \perp\!\!\!\perp Y_i \mid T_i$ , fails despite that  $U$  is not a confounder when either

$$\theta_T \not\perp\!\!\!\perp \theta_U, \theta_T \not\perp\!\!\!\perp \theta_Y \text{ or } \theta_U \not\perp\!\!\!\perp \theta_Y.$$

These are shown in Figure 7, where the open path such that  $T_j \not\perp\!\!\!\perp Y_i \mid T_i$  is marked in red. Note that the direction of the edges between the mechanisms does not influence our conclusion.

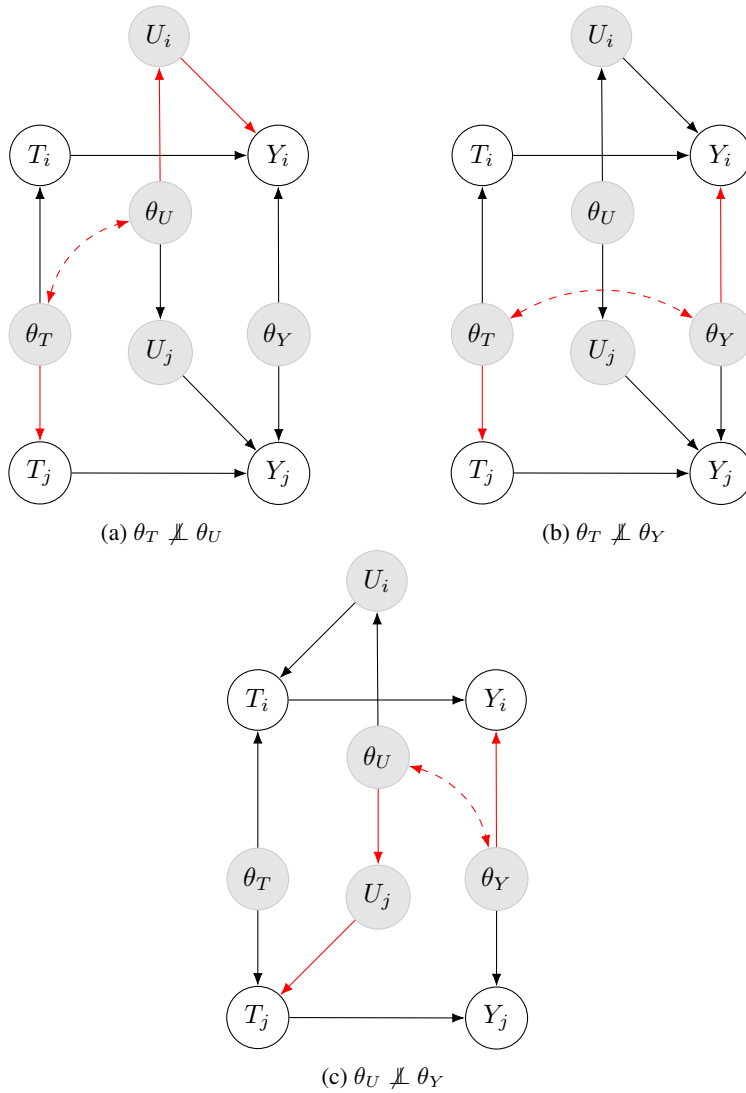


Figure 7: Violations of  $T_j \perp\!\!\!\perp Y_i \mid T_i$  with dependent mechanisms; open paths are marked in red.

## B.2 Degenerate mechanisms

What happens if one or more of the distributions  $P(\theta_T)$ ,  $P(\theta_U)$  and  $P(\theta_Y)$  are constant across all environments? We investigate these scenarios by first adding  $\theta_T$ ,  $\theta_U$  and/or  $\theta_Y$  to the conditioning set of the independencies in Theorem 1. This is done using the same procedure as for proving the theorem, for which the results are displayed in Table 1 (from the seventh column and continuing to the right).

We identify three cases where Theorem 1 fails: when either  $\{\theta_T, \theta_U\}$ ,  $\{\theta_U, \theta_Y\}$  or  $\{\theta_T, \theta_U, \theta_Y\}$  are degenerate together. The reason  $\theta_T$  and  $\theta_U$  can not be degenerate together is that  $T_j \perp\!\!\!\perp Y_i \mid T_i$  no longer exclusively is violated when there is confounding. Similarly, the same happens to  $T_j \perp\!\!\!\perp Y_i \mid Y_i$  when  $\theta_U$  and  $\theta_Y$  are degenerate together.

For Corollary 1, where only the independence  $T_j \perp\!\!\!\perp Y_i \mid T_i$  is used, we note that it is sufficient for just  $\theta_T$  or  $\theta_U$  to be non-degenerate.

## B.3 Faithfulness violation

In this section, we first derive the condition for faithfulness violation that was presented in Example 1. We also include additional insights from the asymptotic behavior of the linear-Gaussian data when the confounder effect sizes – that is  $\gamma$  and  $\lambda$  in (3) – become very large. Lastly, we describe the experimental details on how we produced Figure 4 that illustrated the faithfulness violation in the finite-sample setting.

**Derivation of faithfulness violation** We consider the structural causal model

$$\begin{aligned} U &= \theta_U + \varepsilon_U, & \varepsilon_U &\sim \text{Normal}(0, \sigma_U^2), \\ T &= \gamma U + \theta_T + \varepsilon_T, & \varepsilon_T &\sim \text{Normal}(0, \sigma_T^2), \\ Y &= \lambda U + \beta T + \theta_Y + \varepsilon_Y, & \varepsilon_Y &\sim \text{Normal}(0, \sigma_Y^2), \end{aligned} \quad (3)$$

where  $\theta_T \sim \text{Normal}(0, \sigma_{\theta_T}^2)$ ,  $\theta_U \sim \text{Normal}(0, \sigma_{\theta_U}^2)$  and  $\theta_Y \sim \text{Normal}(0, \sigma_{\theta_Y}^2)$ . We have that  $\varepsilon_c \perp\!\!\!\perp \theta_c$  for  $c = T, Y, U$ . Now, we want to prove that  $T_j \perp\!\!\!\perp Y_i \mid T_i$  for any  $i \neq j$  when  $\sigma_{\theta_U} = \frac{\sigma_U}{\sigma_T} \sigma_{\theta_T}$ . Note that, compared to (1), we have introduced additional parameters  $\lambda$  and  $\beta$ .

Crucially, we note that the partial correlation

$$\rho_{T_j, Y_i \cdot T_i} = \frac{\rho_{T_j, Y_i} - \rho_{T_j, T_i} \rho_{T_i, Y_i}}{\sqrt{1 - \rho_{T_j, T_i}^2} \sqrt{1 - \rho_{T_i, Y_i}^2}}, \quad (4)$$

is zero if and only if  $T_j \perp\!\!\!\perp Y_i \mid T_i$  when the data is jointly Gaussian (Baba et al., 2004), which is the case for (3) because  $p(T, Y, U) = P(Y \mid T, U)P(T \mid U)P(U)$  where each factor is a Gaussian density.

To check when the partial correlation is zero, we need to find out when

$$\rho_{T_j, Y_i} - \rho_{T_j, T_i} \rho_{T_i, Y_i} = 0.$$

Since  $\rho_{X, Y} = \frac{\text{Cov}(X, Y)}{\sqrt{\text{Var}(X)\text{Var}(Y)}}$  for some random variables  $X$  and  $Y$ , we can write this as

$$\rho_{T_j, Y_i} - \rho_{T_j, T_i} \rho_{T_i, Y_i} = \frac{\text{Cov}(T_j, Y_i)}{\sqrt{\text{Var}(T_j)\text{Var}(Y_i)}} - \frac{\text{Cov}(T_j, T_i)}{\sqrt{\text{Var}(T_j)\text{Var}(T_i)}} \frac{\text{Cov}(T_i, Y_i)}{\sqrt{\text{Var}(T_i)\text{Var}(Y_i)}} \quad (5)$$

$$= \frac{\text{Var}(T_i)\text{Cov}(T_j, Y_i) - \text{Cov}(T_j, T_i)\text{Cov}(T_i, Y_i)}{\sqrt{\text{Var}(T_i)^3\text{Var}(Y_i)}}, \quad (6)$$

where we used the fact that  $\text{Var}(T_i) = \text{Var}(T_j)$  for any samples  $i$  and  $j$ .

First, we need to determine all the (co)variances, for which we need to know

$$\begin{aligned} T_i &= \gamma \theta_U + \gamma \varepsilon_{U, i} + \theta_T + \varepsilon_{T, i} \\ Y_i &= \lambda \theta_U + \lambda \varepsilon_{U, i} + \beta \gamma \theta_U + \beta \gamma \varepsilon_{U, i} + \beta \theta_T + \beta \varepsilon_{T, i} + \theta_Y + \varepsilon_{Y, i} \end{aligned}$$

where the subscript  $i$  of the noise variables indicates that they may take different values for different samples. Also note that  $\mathbb{E}[T_i] = \mathbb{E}[Y_i] = 0$ . Consequently, we can write out the covariances, for any  $i, j$ , as follows:

$$\begin{aligned}\text{Cov}(T_j, Y_i) &= \mathbb{E}[T_j Y_i] = (\gamma\lambda + \beta\gamma^2)\mathbb{E}[\theta_U^2] + \beta\mathbb{E}[\theta_T^2] \\ \text{Cov}(T_j, T_i) &= \mathbb{E}[T_j T_i] = \gamma^2\mathbb{E}[\theta_U^2] + \mathbb{E}[\theta_T^2] \\ \text{Cov}(T_i, Y_i) &= \mathbb{E}[T_i Y_i] = (\gamma\lambda + \beta\gamma^2)\mathbb{E}[\theta_U^2] + (\gamma\lambda + \beta\gamma^2)\mathbb{E}[\varepsilon_U^2] + \beta\mathbb{E}[\theta_T^2] + \beta\mathbb{E}[\varepsilon_T^2] \\ \text{Var}(T_i) &= \mathbb{E}[T_i T_i] = \gamma^2\mathbb{E}[\theta_U^2] + \gamma^2\mathbb{E}[\varepsilon_U^2] + \mathbb{E}[\theta_T^2] + \mathbb{E}[\varepsilon_T^2] \\ \text{Var}(Y_i) &= \mathbb{E}[Y_i Y_i] = 2(\lambda^2 + \beta^2\gamma^2)\mathbb{E}[\theta_U^2] + 2(\lambda^2 + \beta^2\gamma^2)\mathbb{E}[\varepsilon_U^2] + \beta^2\mathbb{E}[\theta_T^2] + \beta^2\mathbb{E}[\varepsilon_T^2] + \mathbb{E}[\theta_Y^2] + \mathbb{E}[\varepsilon_Y^2]\end{aligned}$$

Now, we look at the numerator in (6) and we want to know when it could be zero, since that makes the partial correlation zero:

$$\begin{aligned}0 &= \text{Var}(T_i)\text{Cov}(T_j, Y_i) - \text{Cov}(T_j, T_i)\text{Cov}(T_i, Y_i) \\ &= \gamma\lambda(\mathbb{E}[\theta_U^2]\mathbb{E}[\varepsilon_T^2] - \mathbb{E}[\varepsilon_U^2]\mathbb{E}[\theta_T^2])\end{aligned}$$

The solution is given by

$$\sigma_{\theta_U} = \frac{\sigma_U}{\sigma_T} \sigma_{\theta_T},$$

where the square root of the second moments are equal to the standard deviations. This is the same equality as demonstrated in the example.

**Asymptotic behavior of partial correlation** We also look at the partial correlation and ask what happens when the confounder effect sizes  $\gamma$  or  $\lambda$  become very large. The numerator in (6) grows linearly with respect to both  $\gamma$  and  $\lambda$ , and the other variances can be rewritten as

$$\begin{aligned}\text{Cov}(T_j, T_i) &= \gamma^2\mathbb{E}[\theta_U^2] + O(1) \\ \text{Cov}(T_i, Y_i) &= (\gamma\lambda + \beta\gamma^2)(\mathbb{E}[\theta_U^2] + \mathbb{E}[\varepsilon_U^2]) + O(1) \\ \text{Var}(T_i) &= \gamma^2(\mathbb{E}[\theta_U^2] + \mathbb{E}[\varepsilon_U^2]) + O(1) \\ \text{Var}(Y_i) &= 2(\lambda^2 + \beta^2\gamma^2)(\mathbb{E}[\theta_U^2] + \mathbb{E}[\varepsilon_U^2]) + O(1)\end{aligned}$$

where  $O(1)$  is a constant with respect to  $\gamma$  and  $\lambda$ .

We rewrite the partial correlation (4) as

$$\rho_{T_j, Y_i, T_i} = \frac{(\text{Var}(T_i)\text{Cov}(T_j, Y_i) - \text{Cov}(T_j, T_i)\text{Cov}(T_i, Y_i)) / \sqrt{\text{Var}(T_i)^3 \text{Var}(Y_i)}}{\sqrt{1 - \frac{\text{Cov}(T_j, T_i)^2}{\text{Var}(T_i)^2}} \sqrt{1 - \frac{\text{Cov}(T_i, Y_i)^2}{\text{Var}(T_i)\text{Var}(Y_i)}}}.$$

Assuming that all second moments are non-zero and finite, it is possible to show that

$$\rho_{T_j, Y_i, T_i} \propto \begin{cases} \gamma^{-3} & \text{for } |\gamma| \gg 1, \\ 1 & \text{for } |\lambda| \gg 1. \end{cases}$$

Hence, when either  $|\gamma|$  or  $|\lambda|$  goes to infinity we have

$$\begin{aligned}\rho_{T_j, Y_i, T_i} &\xrightarrow{|\gamma| \rightarrow \infty} 0 \\ \rho_{T_j, Y_i, T_i} &\xrightarrow{|\lambda| \rightarrow \infty} C \text{ for some } C \in [-1, 1]\end{aligned}$$

Note that  $C$  could be zero, for instance when  $\sigma_{\theta_U} = \frac{\sigma_U}{\sigma_T} \sigma_{\theta_T}$ , although we demonstrate with simulation studies in Appendix C a case where  $C$  is non-zero as well.

Interestingly, in this case, the bias from estimating the causal effect without adjusting for the confounder  $U$  is

$$\mathbb{E}[Y | do(T)] - \mathbb{E}[Y | T] = \beta T - \left(\beta T + \frac{\lambda}{\gamma} T\right) = -\frac{\lambda}{\gamma} T.$$

We note that when  $\gamma \rightarrow \infty$  the bias goes to zero, similar to the partial correlation. Meanwhile, the bias increases with  $\lambda$  which also is consistent with the asymptotic behavior of the partial correlation as  $\lambda \rightarrow \infty$ .

**Experimental details** We describe the experiment that illustrated the faithfulness violation in Figure 4. We generate data according to (3) with the following parameters fixed:  $\beta = \gamma = \lambda = 1$ ,  $\sigma_{\theta_Y} = 1$ ,  $\sigma_Y = \sigma_U = 1$  and  $\sigma_T = \frac{2}{3}$ . Meanwhile, we vary  $\sigma_{\theta_T}$  and  $\sigma_{\theta_U}$  between 0 and 5. We test  $T_j \perp\!\!\!\perp Y_i \mid T_i$  using the partial correlation (Baba et al., 2004). The experiment is repeated 1000 times with 1000 environments and a significance level  $\alpha = 0.05$ .

## C Additional experiments

We present additional simulation studies, mainly replicating the experiments from Section 5 with continuous data. In addition, we further investigate the asymptotic behavior of the partial correlation from Appendix B.3 with both the binary and continuous data.

The continuous data is generated from a linear-Gaussian DAG as described in (3). Unless otherwise stated, we use  $\beta = 1$ ,  $\sigma_T = \sigma_U = \sigma_Y = 1$ ,  $\sigma_{\theta_T} = \sigma_{\theta_Y} = 1$  and  $\sigma_{\theta_U} = 5$ . We test  $T_j \perp\!\!\!\perp Y_i \mid T_i$  using the partial correlation (Baba et al., 2004) with  $N = 2$  samples. Note that the figures for experiments with continuous data looks smoother since we run more iterations for these due to lower computational runtime.

For the first experiment, we vary the number of environments and the confounder effect size (where we set  $\gamma = \lambda$ ) as in Figure 5a, although we increase the range of the confounder effect size up to 15 for this experiment. Similarly, we do the same experiment with the binary data for comparison. The results are seen in Figure 8. Notably, the probability of detecting hidden confounding starts decreasing when  $\gamma = \lambda$  goes above a certain threshold. This is consistent with our previous conclusions from Appendix B.3, where we noted that partial correlation is proportional to  $\gamma^{-3}$  for  $\gamma \gg 1$  while remaining constant for  $\lambda \gg 1$ . Hence, we would expect the partial correlation to shrink as both  $\gamma$  and  $\lambda$  grows. Notably, the effect is more pronounced with the continuous data although it can also be seen with the binary data.

Secondly, we perform a similar to the first one but we only vary  $\lambda$  while fixing  $\gamma = 1$ . The results are shown in in Figure 9, we note that the probability of detection does no longer decrease as the confounder effect size increases. Once again, this is predicted by the asymptotic behavior of the partial correlation.

Finally, we compare our statistical testing procedure to testing  $Y \perp\!\!\!\perp E \mid T$  with continuous data in Figure 10. We run the experiment with 10000 environments, 100 samples per environment and  $\sigma_{\theta_U} = 10$  to avoid the issues of faithfulness violations which we have discussed before. Similar to the case with binary data, we see that the probability of false detection when testing  $Y \perp\!\!\!\perp E \mid T$  grows as the standard deviation of  $\theta_Y$  increases. Meanwhile, we do not observe this problem for our testing procedure.

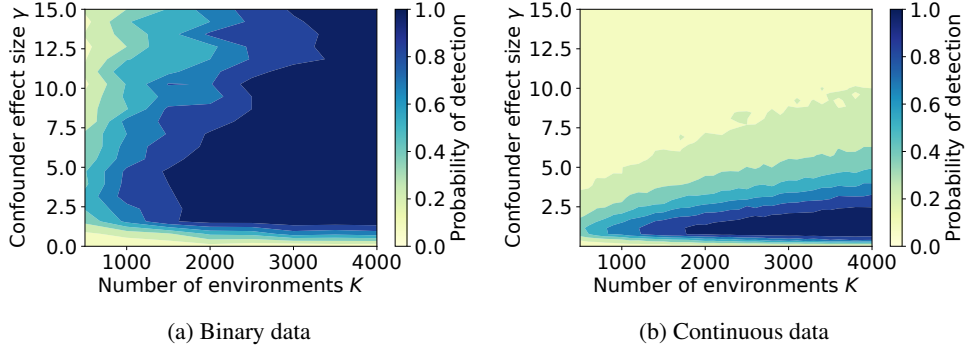


Figure 8: Probability of detecting hidden confounding for varying the number of environments  $K$  and confounder effect sizes where  $\gamma = \lambda$  are equal.

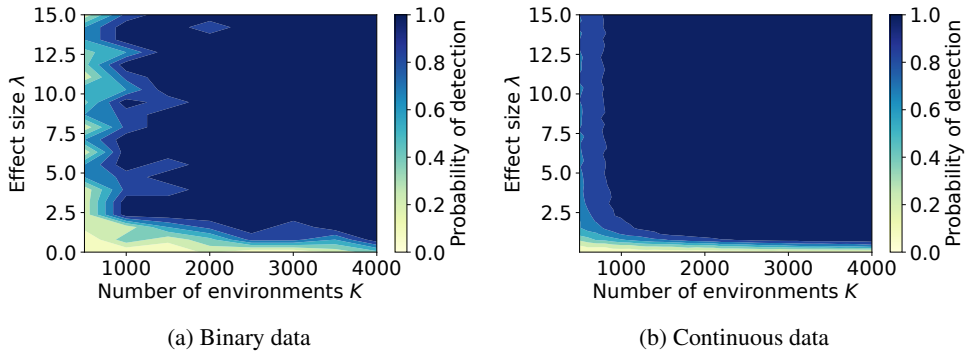


Figure 9: Probability of detecting hidden confounding for varying the number of environments  $K$  and confounder effect sizes where  $\lambda$  is varied while  $\gamma = 1$  fixed.

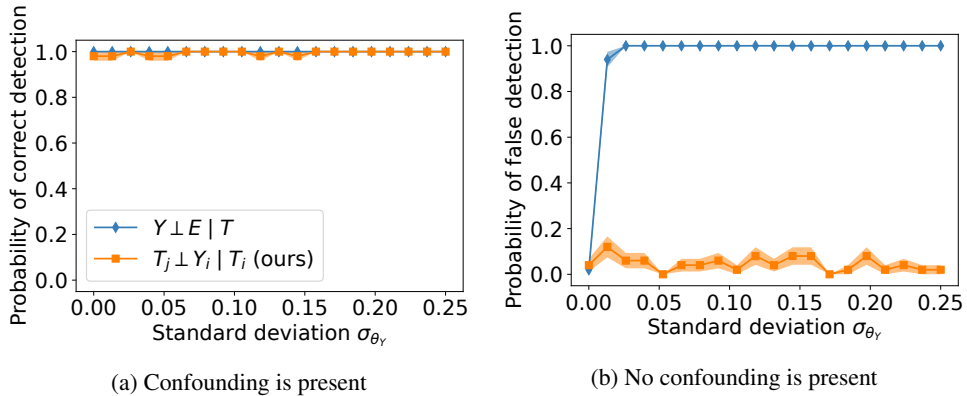


Figure 10: Comparison on linear-Gaussian data between the proposed procedure and an alternative testing procedure by varying the standard deviation of  $\theta_Y$  in both the presence and absence of confounding.

## D Algorithms

In this section, we present the algorithms corresponding to the two statistical testing procedure described in Section 4.3: the asymptotic G-test procedure (McDonald, 2014) and Monte-Carlo permutation based procedure (Tsamardinos and Borboudakis, 2010).

---

### Algorithm 1: Asymptotically correct testing procedure

---

**Input:** Categorical data  $\{(T_{i,k}, Y_{i,k})\}_{i=1}^N$  from environments  $k = 1, \dots, K$ ; significance level  $\alpha$

**if**  $N$  is even **then**  
 |  $L \leftarrow N/2$  Split up data into  $L$  two-sample pairs  
**else**  
 |  $L \leftarrow (N - 1)/2$

**for**  $i = 1, \dots, L$  **do**  
 |  $G_{statistic}^{(i)} \leftarrow \text{G-test}(T_{2i-1,\cdot} \perp\!\!\!\perp Y_{2i,\cdot} \mid T_{2i,\cdot})$  Compute G-test statistic for each sample pair

$G_{total} \leftarrow \sum_{i=1}^L G_{statistic}^{(i)}$  Sum up computed test statistics  
 $C_{dof} \leftarrow L \cdot |\mathcal{T}| \cdot (|\mathcal{T}| - 1) \cdot (|\mathcal{Y}| - 1)$  Degrees of freedom  
 $p \leftarrow 1 - \text{cdf}_{\chi^2}(G; C_{dof})$

**return**  $p \leq \alpha$

---



---

### Algorithm 2: Monte-Carlo permutation based testing procedure

---

**Input:** Categorical data  $\{(T_{i,k}, Y_{i,k})\}_{i=1}^N$  from environments  $k = 1, \dots, K$ ; significance level  $\alpha$ ; number of permutations  $C$

**if**  $N$  is even **then**  
 |  $L \leftarrow N/2$  Split up data into  $L$  two-sample pairs  
**else**  
 |  $L \leftarrow (N - 1)/2$

**for**  $i = 1, \dots, L$  **do**  
 |  $G_{statistic}^{(i)} \leftarrow \text{G-test}(T_{2i-1,\cdot} \perp\!\!\!\perp Y_{2i,\cdot} \mid T_{2i,\cdot})$  Compute G-test statistic for each sample pair

$G_{total} \leftarrow \sum_{i=1}^L G_{statistic}^{(i)}$  Sum up computed test statistics

**for**  $j = 1, \dots, C$  **do**  
 | **for**  $i = 1, \dots, L$  **do**  
 | |  $u \leftarrow \text{Unif}(0, 1)$  Randomly select one of the variables to permute  
 | | **if**  $u < 0.5$  **then**  
 | | |  $A \leftarrow \{T_{2i-1,k}\}_{k=1}^K$   
 | | |  $B \leftarrow \{Y_{2i,k}\}_{k=1}^K$   
 | | | **else**  
 | | |  $B \leftarrow \{T_{2i-1,k}\}_{k=1}^K$   
 | | |  $A \leftarrow \{Y_{2i,k}\}_{k=1}^K$   
 | | | **for**  $t \in \mathcal{T}$  **do**  
 | | | | Permute entries in  $A$  with the same values of  $T_{2i,\cdot} = t$   
 | | |  $G_{tmp}^{(i)} \leftarrow \text{G-test}(A \perp\!\!\!\perp B \mid T_{2i,\cdot})$  Compute statistic from permuted data for sample pair  
 | | | **pair**  
 | |  $G_{perm}^{(j)} = \sum_{i=1}^L G_{tmp}^{(i)}$

$p \leftarrow \sum_{j=1}^C \mathbb{1}_{G_{perm}^{(j)} > G_{total}} / C$  Approximate p-value

**return**  $p \leq \alpha$

---